Key Points:
- The Hadley circulation extent and strength are analyzed in simulations spanning the Last Glacial Maximum to global warming scenarios
- The Hadley circulation generally widens and weakens as the climate warms
- Changes in meridional temperature gradients have a modest modulating effect, principally on the Southern Hemisphere Hadley circulation

Correspondence to:
R. D'Agostino,
roberta.dagostino@mpimet.mpg.de

Factors controlling Hadley circulation changes from the Last Glacial Maximum to the end of the 21st century

Roberta D'Agostino[1,2,3], Piero Lionello[2,3] (ID), Ori Adam[4,5] (ID), and Tapio Schneider[4,6] (ID)

[1]Max Planck Institute for Meteorology, Hamburg, Germany, [2]DiSTeBA, University of Salento, Lecce, Italy, [3]Euro-Mediterranean Center on Climate Change, Lecce, Italy, [4]Geological Institute, ETH Zurich, Switzerland, [5]Hebrew University, Jerusalem, Israel, [6]California Institute of Technology, Pasadena, California, USA

Abstract The Hadley circulation (HC) extent and strength are analyzed in a wide range of simulated climates from the Last Glacial Maximum to global warming scenarios. Motivated by HC theories, we analyze how the HC is influenced by the subtropical stability, the near-surface meridional potential temperature gradient, and the tropical tropopause level. The subtropical static stability accounts for the bulk of the HC changes across the simulations. However, since it correlates strongly with global mean surface temperature, most HC changes can be attributed to global mean surface temperature changes. The HC widens as the climate warms, and it also weakens, but only robustly so in the Northern Hemisphere. On the other hand, the Southern Hemisphere strength response is uncertain, in part because subtropical static stability changes counteract meridional potential temperature gradient changes to various degrees in different models, with no consensus on the response of the latter to global warming.

1. Introduction

Simulations of greenhouse gas (GHG)-induced global warming consistently point to a widening of the Hadley circulation (HC) as the climate warms, which has been suggested to be linked to an increase of the subtropical static stability [*Walker and Schneider*, 2006; *Frierson et al.*, 2007; *Lu et al.*, 2007, 2008]. Such a widening has also been observed in recent decades [*Hu and Fu*, 2007; *Seidel et al.*, 2008; *Birner*, 2010; *Davis and Rosenlof*, 2012; *Nguyen et al.*, 2013; *Adam et al.*, 2014; *D'Agostino and Lionello*, 2017]. However, what causes these changes has not been clearly established. A substantial fraction of recent HC variations are not related to changes in subtropical static stability: The HC narrows as meridional temperature gradients strengthen, as seen under El Niño [e.g., *Lu et al.*, 2008; *Adam et al.*, 2014]. It expands and weakens as meridional temperature gradients weaken, for example, in GHG-induced global warming scenarios [*Seo et al.*, 2014] and under La Niña conditions [*Lu et al.*, 2008].

In angular momentum-conserving theories [*Held and Hou*, 1980], the HC extent depends on meridional temperature gradients but not on the static stability. However, Earth's HC usually is not close to the angular momentum-conserving limit [*Walker and Schneider*, 2006; *Schneider*, 2006]. Instead, especially near the subtropical HC edges where Rossby numbers are generally small, the direction of the upper tropospheric meridional mass flux is controlled by the sign of the eddy momentum flux divergence. Because the eddy momentum fluxes are baroclinically generated, this opens up the possibility that the HC extent and strength depend on baroclinicity measures, which generally involve the isentropic slope and thus depend on meridional temperature gradients, the static stability, and generally also the tropopause level [*Held*, 2000; *Schneider*, 2006; *Schneider et al.*, 2010]. Indeed, the HC extent and strength have been quantitatively linked to factors such as the static stability, meridional temperature gradients, and the tropopause level in wide ranges of dry and moist idealized general circulation model studies [*Schneider and Walker*, 2008; *Korty and Schneider*, 2008; *O'Gorman*, 2011; *Levine and Schneider*, 2015].

Motivated by such theories of the HC, here we analyze the relationship of HC changes to variations in subtropical static stability, meridional temperature gradients, mean temperature, and tropopause level in a wide range of simulated climates within the Paleoclimate Modelling Intercomparison Project Phase 3 (PMIP3) and from the Coupled Model Intercomparison Project Phase 5 (CMIP5). This approach allows us to test theories of the HC response to climate change under a broader range of conditions than considered previously.

We include simulations of GHG warming, as most previous studies did [*Lu et al.*, 2007, 2008; *Seo et al.*, 2014], and also simulations with changes in orbital parameters and ice cover.

2. Data and Methods

We use monthly PMIP3 and CMIP5 data from the Last Glacial Maximum (LGM), Mid-Holocene (MIDH), Pre-Industrial Control (PIC), Historical (HIST), and Representative Concentration Pathways 4.5 and 8.5 (RCP4.5 and RCP8.5) experiments. For each of these experiments, we use the first ensemble member (r1i1p1) of available models (Table S1 in the supporting information). All data sets are zonally averaged and interpolated to 1° latitude resolution.

Analysis is based on the meridional mass stream function:

$$\psi = \frac{2\pi a \cos \phi}{g} \int_0^p v \, dp \, , \tag{1}$$

where v is the zonal mean meridional wind component, p is pressure, g is the gravitational acceleration, a is Earth's radius, and ϕ is latitude. As an index of HC extent, we compute by linear interpolation the subtropical zero-crossing latitude of ψ averaged between the 300 and 700 hPa levels. As an index of HC strength, we use the stream function maximum in the Northern Hemisphere (NH) and minimum in the Southern Hemisphere (SH) between the 100 and 700 hPa levels and equatorward of 30°. We use absolute values for the indices of NH and SH HC extent (ϕ_{NH} and ϕ_{SH}) and strength (ψ_{NH} and ψ_{SH}).

Climatologies are calculated for the last 30 years of the RCP experiments, for the years 1979–2004 of the HIST experiment, for the full length of the PIC time series, and over 200 years centered at year 1000 for MIDH and LGM. We examine the covariance of the HC extent and strength with the following factors:

1. The first factor is the tropical mean surface temperature ($\langle TT \rangle$) equatorward of 30°. Here we use $\langle TT \rangle$ instead of the global mean surface temperature to minimize effects of enhanced continental warming and ice sheet cover changes. However, results based on global mean temperature do not differ qualitatively from those based on $\langle TT \rangle$, as their correlation is very high ($R = 0.96$, 5% significance level, Student's t test).
2. The second factor is the meridional near-surface (averaged between the 700 and 800 hPa levels) potential temperature contrast ($\Delta_h \theta$), calculated as the difference between the potential temperature in the deep tropics (equatorward of 10°) and the extratropics (between 40° to 60° in each hemisphere).
3. The third factor is the subtropical near-surface static stability ($\Delta_v \theta$), defined as the potential temperature difference between the 700 and 800 hPa levels and averaged between 20° and 40° latitude in each hemisphere.
4. The last factor is the tropical (15°S–15°N) tropopause pressure level (p_t), calculated as the lowest level at which the lapse rate drops below 2 K km^{-1}, following the method described in *Birner* [2010].

3. Results

Figure 1 shows the seasonal cycle of HC strength and extent across the climates, computed as the ensemble mean of seasonal cycles in individual models. Across all seasons, both ϕ_{NH} and ϕ_{SH} shift poleward from the coldest (LGM) to the warmest (RCP8.5) experiment. In the NH, the poleward shift is larger in late boreal summer/early fall than in the winter, while in the SH it is approximately constant throughout the year. In the NH, the month in which the maximum northward extent is reached shifts progressively later in the year as the climate warms, being delayed by about 1 month in the warmest relative to the coldest climate. This likely reflects the tendency for a delayed retreat of the Northern Hemisphere summer monsoons under global warming [*Kitoh et al.*, 2013]. The winter and summer HC generally weaken with global warming in both hemispheres, roughly in proportion to their climatological mean strength. The NH winter HC is strongest and narrowest in LGM. In contrast, the SH winter HC is strongest and narrowest in MIDH. This suggests that interhemispheric temperature differences (which are maximal during NH winter in LGM and during SH winter in MIDH, see Figure S1) can modulate HC extent and strength [*Chiang and Friedman*, 2012].

Since HC strength variations are most significant in winter, and since HC extent variations are consistent across all seasons, here we focus on winter HC variations. Analysis of summer HC variations is provided in the supporting information.
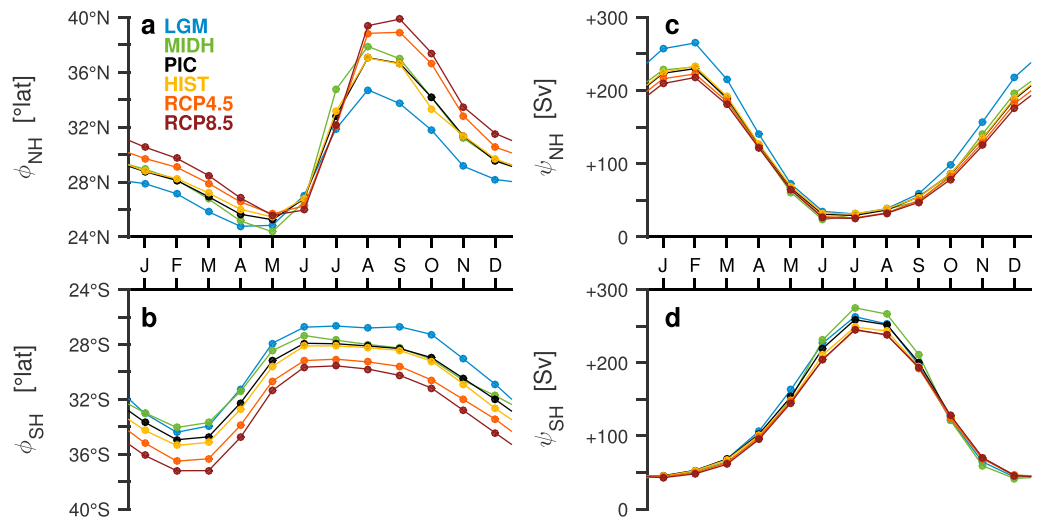
Figure 1. Seasonal cycle of the multimodel ensemble mean (a) ϕ_{NH}, (b) ϕ_{SH}, (c) ψ_{NH}, and (d) ψ_{SH}. Experiment color codes are listed in Figure 1a for LGM (ensemble mean $\langle TT \rangle$ = 294.0 K), MIDH (296.5 K), PIC (296.9 K), HIST (297.4 K), RCP4.5 (299.0 K), and RCP8.5 (300.6 K).

Figure 2 shows the multimodel mean winter stream function difference in the LGM, MIDH, and RCP8.5 scenarios relative to PIC. The PIC multimodel mean was calculated separately for LGM, MIDH, and RCP8.5, accounting for the different model ensembles in each experiment. However, this does not affect results significantly, as shown by the similarity of the reference PIC stream functions (black contours) in the three columns. The HC shows opposite behaviors between the coldest (LGM) and the warmest (RCP8.5) experiment: in both hemispheres, the HC shifts poleward and weakens and the tropopause pressure level decreases (height increases) with global warming, as was shown in previous studies [*Diaz and Bradley*, 2004; *Schneider*, 2004; *Otto-Bliesner and Clement*, 2004; *Schneider*, 2007; *Braconnot et al.*, 2007]. On the other hand, the HC in MIDH differs substantially from both LGM and RCP8.5, with a northward displacement and weakening of the NH HC relative to PIC in austral winter and little change in boreal winter.
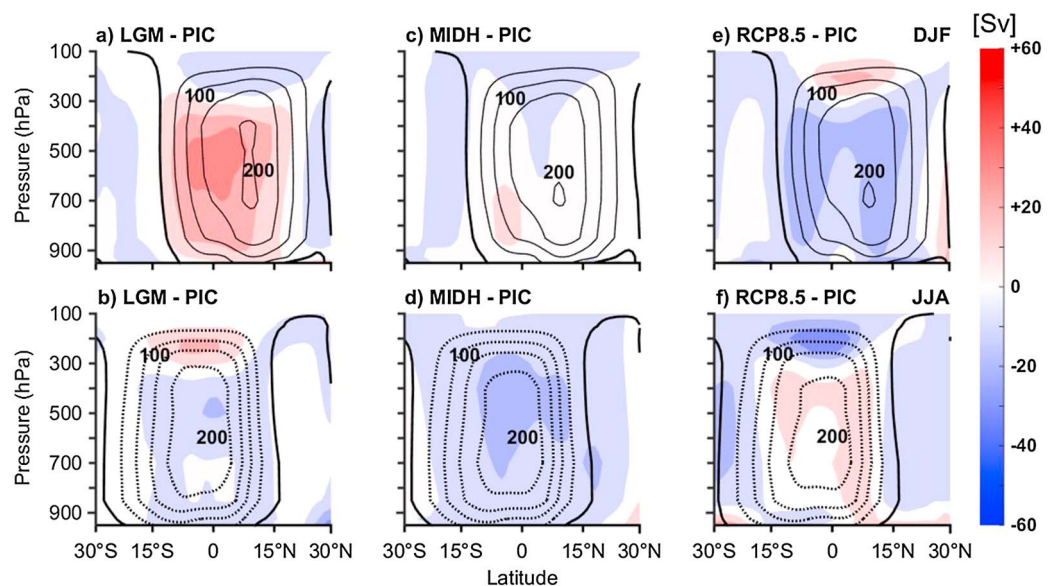

Figure 2. Multimodel ensemble mean stream function difference between LGM, MIDH, and RCP8.5 and relative to PIC. In each panel, the difference is indicated by filled colors (contour interval 10 Sv, 1 Sv = 10^9 kg s^{-1}) for December–February (a, c, and e) and June–August (b, d, and f). Black contours show the PIC reference stream function: dashed (solid) lines indicate negative (positive) values of the stream function (contour interval 40 Sv).
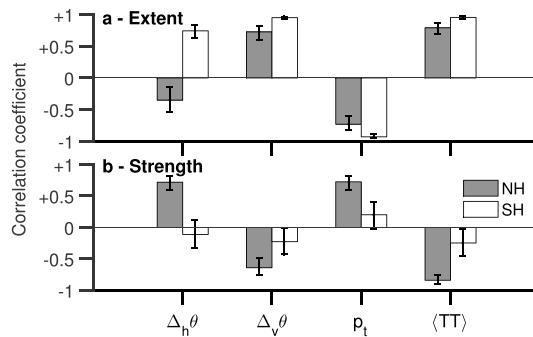
Figure 3. Correlation coefficients across the collection of simulations (Figures S2 and S3) between winter values of (a) ϕ_{NH} and ϕ_{SH} and (b) ψ_{NH} and ψ_{SH} with $\Delta_h\theta$, $\Delta_v\theta$, p_t, and $\langle TT \rangle$ in the NH (gray bars) and SH (white bars). Error bars show lower and upper bounds for a 95% confidence interval for each correlation coefficient.

In order to identify the dominant mechanisms leading to HC changes, we compute the linear regression coefficients of the HC extent and strength on factors associated with theories of the HC. To reduce the sensitivity of our results to variability in the mean states of the climate models, we base our analysis on deviations from the PIC experiment, denoted by δ and computed separately for each climate model. Robust regressions are used to reduce sensitivity to outliers [*Huber*, 1981]. Figure 3 shows the correlation coefficients and their error bars based on the scatter plots in supporting information Figures S2 and S3. They indicate a consistent relation of the HC in both hemispheres with subtropical static stability $\Delta_v\theta$ and tropopause level p_t. The HC widens and weakens as the subtropical static stability increases and as the tropical tropopause pressure level decreases. Both factors explain a comparable amount of ϕ_{NH}, ϕ_{SH}, ψ_{NH}, and ψ_{SH} variance (Table 2). However, they are themselves strongly correlated (Table 1) and therefore cannot be regarded as independent predictors. Additional details for specific models and intermodel spread are provided in Figures S2 and S3.

The dependence of HC extent and strength on $\Delta_h\theta$ differs between the hemispheres. In the SH, $\Delta_h\theta$ increases with global warming, while in the NH it decreases, primarily because $\Delta_h\theta$ increases in the NH in the LGM simulations as a result of ice cover changes. In general, identifying how much the HC strength in the SH (ψ_{SH}) is influenced by the various factors we considered is made difficult by its weak overall change with global warming. Note that the opposite signs of the correlation of $\Delta_h\theta_{SH}$ and $\Delta_h\theta_{NH}$ with $\langle TT \rangle$, on one hand, and the weak correlation of ψ_{SH} with all factors (Figure 3b and Table 2), with large error bars reflecting the large scatter among simulations, reinforce these statements.

As shown in Table 1, all factors are strongly correlated with the tropical temperature $\langle TT \rangle$. Figure 4 show scatterplots of ϕ_{NH}, ϕ_{SH}, ψ_{NH}, and ψ_{SH}, all versus $\langle TT \rangle$. The HC edges shift poleward with increasing $\langle TT \rangle$ in both hemispheres at a similar rate of 0.35°/K. The HC weakens with increasing $\langle TT \rangle$ only in the NH, at a rate of 6 sverdrup (Sv)/K. The SH exhibits a large intermodel spread, with 50% of the models showing a strengthening of the SH HC under warming. Variations of tropical temperatures $\langle TT \rangle$ alone can explain 62% of the wintertime variance in the NH strength ϕ_{NH}, 90% of ϕ_{SH}, 71% of ψ_{NH}, and 6% of ψ_{SH}. Results during the summer do not differ qualitatively from winter, except for the NH summer HC, which robustly contracts equatorward with global warming, as a result of a seasonality change (Figure S4).

Since the various factors cannot easily be isolated because of their strong correlations, we evaluate the combined contribution of the factors in a multiple regression model using $\Delta_h\theta$, $\Delta_v\theta$, and p_t as predictors.

Table 1. Mutual Winter Correlations (R) Between Tropical Surface Temperature ($\langle TT \rangle$), Meridional Temperature Gradient ($\Delta_h\theta$), Subtropical Static Stability ($\Delta_v\theta$), and Tropical Tropopause (p_t), for the NH (Above Diagonal) and SH (Below Diagonal)[a]

R	$\langle TT \rangle$	$\Delta_h\theta$	$\Delta_v\theta$	p_t
$\langle TT \rangle$	–	−0.57	+0.85	−0.93
$\Delta_h\theta$	+0.59	–	−0.54	+0.49
$\Delta_v\theta$	+0.97	+0.55	–	−0.92
p_t	−0.93	−0.52	−0.92	–

[a]All correlations are significant (5% significance level, Student's t test).

Table 2. Explained Variance (R^2) For Regression Models of ϕ_{NH}, ϕ_{SH}, ψ_{NH}, and ψ_{SH} on $\Delta_h\theta$, $\Delta_v\theta$, p_t, and $\langle TT\rangle$[a]

R^2	ϕ_{NH}	ϕ_{SH}	ψ_{NH}	ψ_{SH}
$\Delta_h\theta$	13%	50%	54%	1%
$\Delta_v\theta$	54%	90%	41%	5%
p_t	54%	86%	52%	4%
$\langle TT\rangle$	62%	90%	71%	6%
Three predictors	60% (58%)	93% (93%)	79% (78%)	18% (15%)

[a]The last line shows results of a multiple regression model using $\Delta_h\theta$, $\Delta_v\theta$, and p_t as predictors. Adjusted variance (R^2_{adj}), accounting for the increased degrees of freedom in the multiple regression model, is shown in parentheses.

As expected, this model does improve the total explained variance relative to the simple regressions (Table 2) for each predictor, although for ψ_{SH}, a large fraction of the total variance remains unaccounted for even in the multiple regression model. Similar results are obtained for regression analyses with only two predictors. From the R^2 values in Table 2, it is evident that $\langle TT\rangle$ is the single best predictor of HC extent and strength in both hemispheres, with a predictive power comparable to that of the multiple regression model. Likely, this arises because increases in latent heat release in warmer climates lead to an increased static stability [*Schneider and O'Gorman*, 2008], and the tropopause height increases with warming as implied by radiative-convective considerations [*Schneider*, 2007]. This leads to strong correlations among mean temperature, static stability, and tropopause level. Both the static stability and tropopause level naturally arise in theories for HC extent and strength [*Schneider et al.*, 2010]. But notwithstanding the strong correlation of $\langle TT\rangle$ with HC extent and strength, it is unlikely that mean temperature itself should enter HC theories explicitly, for example, because in dry atmospheres, the mean temperature can only affect dynamics through its nonlinear effects on radiative transfer.
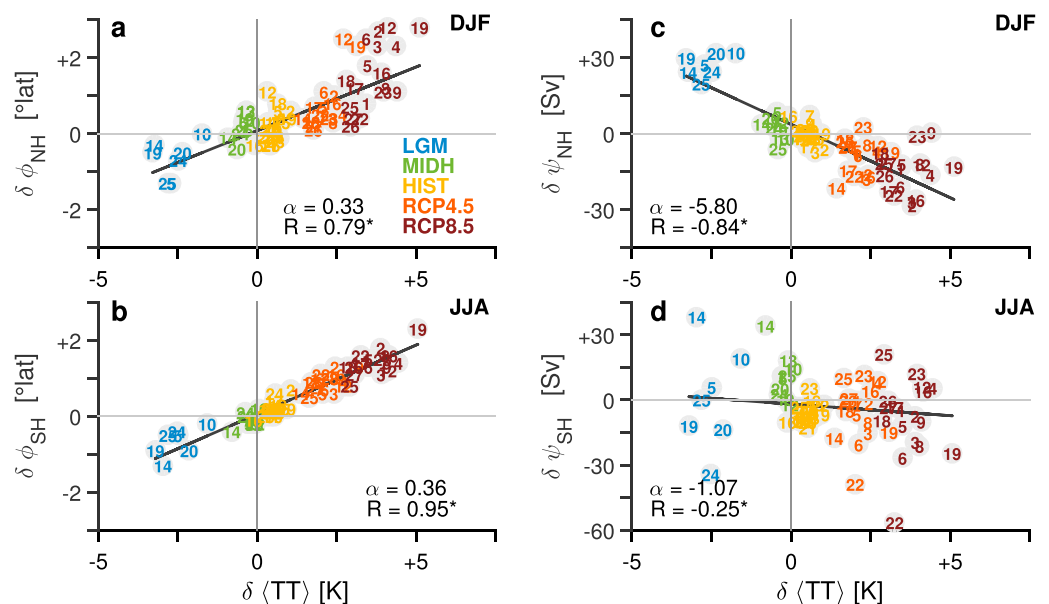

Figure 4. Relation of winter values of $\langle TT\rangle$ with (a) ϕ_{NH}, (b) ϕ_{SH}, (c) ψ_{NH}, and (d) ψ_{SH}. What is plotted are differences from PIC (denoted by δ). Experiments are identified by different colors, following the legend listed in Figure 4a. Each model is marked by a number, as in Table S1. Robust regressions over the whole collection of models are indicated by black lines. Regression coefficients (α) and correlation coefficients (R) are listed inside each panel. Statistically significant correlations (5% significance level, Student's t test) are indicated by an asterisk.

4. Conclusions

We investigated the HC extent and strength in a wide range of PMIP3 and CMIP5 climate simulations, ranging from LGM to RCP8.5 experiments. The wide range of climate variations allowed us to extract robust results on HC variations, including the GHG induced changes on which previous studies have focused [*Lu et al.*, 2007; *Seo et al.*, 2014].

We found that changes in subtropical static stability, meridional temperature gradients, and tropical tropopause level are all strongly correlated with the tropical mean temperature across models and experiments. Tropical temperature therefore emerged as the best predictor of HC variations across the range of simulations we considered. Consistent with previous studies, we found that the HC widens as the tropical temperature increases, at a rate of ∼0.7°/K on average. This is of similar magnitude but slightly higher than the rate calculated for the Intergovernmental Panel on Climate Change-Fourth Assessment Report (AR4) high-emission scenario (∼0.6°/K) [*Lu et al.*, 2007], but lower than that calculated taking into account only CMIP5 HIST simulations (∼1°/K) [*Adam et al.*, 2014].

The HC generally weakens with global warming, by up to about 4%/K, which can be compared with the multimodel ensemble-mean of 1.2%/K calculated for the AR4 high-emission scenario [*Lu et al.*, 2007; *Vecchi and Soden*, 2007]. The weakening occurs in all seasons, but it is more significant in the NH. The HC weakens at a rate of about 6 Sv/K and 2 Sv/K in the NH winter and summer, respectively, but by only 1 Sv/K and 0.8 Sv/K in the SH winter and summer. The relatively small HC strength change in the SH hides substantial variations across models: about half of the models show a strengthening and half a weakening of the SH HC. Some of the scatter across models depends on the degree of compensation between effects of changes in the subtropical static stability and in the near-surface meridional potential temperature contrast, which decreases in most models but increases in some. However, even the multiple regression model accounts for only a small fraction of the variations across models. This suggests that other factors than those we considered are important for accounting for the variations in SH HC strength and its scatter across models.

Our analysis suggests that subtropical static stability changes, which correlate strongly with tropical and global mean surface temperature changes, account for the most of the HC changes. Tropical temperature therefore emerges as a good predictor in these climate change experiments. However, in other climate changes, for example, in which mean temperature changes and changes in meridional temperature gradients decouple, the meridional temperature gradient and other factors may exert a greater independent influence on the HC.

References

Adam, O., T. Schneider, and N. Harnik (2014), Role of changes in mean temperatures versus temperature gradients in the recent widening of the Hadley circulation, *J. Clim.*, *27*(19), 7450–7461.

Birner, T. (2010), Recent widening of the tropical belt from global tropopause statistics: Sensitivities, *J. Geophys. Res.*, *115*, D23109, doi:10.1029/2010JD014664.

Braconnot, P., et al. (2007), Results of PMIP2 coupled simulations of the Mid-Holocene and Last Glacial Maximum—Part 1: Experiments and large-scale features, *Clim. Past*, *3*, 261–277.

Chiang, J. C., and A. R. Friedman (2012), Extratropical cooling, interhemispheric thermal gradients, and tropical climate change, *Annu. Rev. Earth Planet. Sci.*, *40*, 383–412.

D'Agostino, R., and P. Lionello (2017), Evidence of global warming impact on the evolution of the Hadley circulation in ECMWF centennial reanalyses, *Clim. Dyn.*, *48*(9–10), 3047–3060.

Davis, S. M., and K. H. Rosenlof (2012), A multidiagnostic intercomparison of tropical-width time series using reanalyses and satellite observations, *J. Clim.*, *25*(4), 1061–1078.

Diaz, H. F., and R. S. Bradley (2004), *The Hadley Circulation: Present, Past, and Future*, Springer, Netherlands.

Frierson, D. M., J. Lu, and G. Chen (2007), Width of the Hadley cell in simple and comprehensive general circulation models, *Geophys. Res. Lett.*, *34*, L18804, doi:10.1029/2007GL031115.

Held, I. M. (2000), The general circulation of the atmosphere. paper presented at 2000 Program in Geophysical Fluid Dynamics, Woods Hole Oceanographic Institution, Woods Hole, Mass.

Held, I. M., and A. Y. Hou (1980), Nonlinear axially symmetric circulations in a nearly inviscid atmosphere, *J. Atmos. Sci.*, *37*(3), 515–533.

Hu, Y., and Q. Fu (2007), Observed poleward expansion of the Hadley circulation since 1979, *Atmos. Chem. Phys.*, *7*(19), 5229–5236.

Huber, P. (1981), *Robust Statistics*, 308 pp., John Wiley, New York.

Kitoh, A., H. Endo, K. Krishna Kumar, I. F. Cavalcanti, P. Goswami, and T. Zhou (2013), Monsoons in a changing world: A regional perspective in a global context, *J. Geophys. Res. Atmos.*, *118*, 3053–3065, doi:10.1002/jgrd.50258.

Korty, R. L., and T. Schneider (2008), Extent of Hadley circulations in dry atmospheres, *Geophys. Res. Lett.*, *35*, L23803, doi:10.1029/2008GL035847.

Levine, X. J., and T. Schneider (2015), Baroclinic eddies and the extent of the Hadley circulation: An idealized GCM study, *J. Atmos. Sci.*, *72*, 2744–2761.

Lu, J., G. A. Vecchi, and T. Reichler (2007), Expansion of the Hadley cell under global warming, *Geophys. Res. Lett.*, *34*, L06805, doi:10.1029/2006GL028443.

Lu, J., G. Chen, and D. M. Frierson (2008), Response of the zonal mean atmospheric circulation to El Niño versus global warming, *J. Clim.*, *21*(22), 5835–5851.

Nguyen, H., A. Evans, C. Lucas, I. Smith, and B. Timbal (2013), The Hadley circulation in reanalyses: Climatology, variability, and change, *J. Clim.*, *26*(10), 3357–3376.

O'Gorman, P. A. (2011), The effective static stability experienced by eddies in a moist atmosphere, *J. Atmos. Sci.*, *68*, 75–90.

Otto-Bliesner, B. L., and A. Clement (2004), The sensitivity of the Hadley circulation to past and future forcings in two climate models, in *The Hadley Circulation: Present, Past and Future*, edited by H. F. Diaz and R. S. Bradley, pp. 437–464, Springer, Netherlands.

Schneider, T. (2004), The tropopause and the thermal stratification in the extratropics of a dry atmosphere, *J. Atmos. Sci.*, *61*, 1317–1340.

Schneider, T. (2006), The general circulation of the atmosphere, *Annu. Rev. Earth Planet. Sci.*, *34*, 655–688.

Schneider, T. (2007), The thermal stratification of the extratropical troposphere, in *The Global Circulation of the Atmosphere*, edited by T. Schneider and A. H. Sobel, pp. 47–77, Princeton Univ. Press, Princeton, N. J.

Schneider, T., and P. A. O'Gorman (2008), Moist convection and the thermal stratification of the extratropical troposphere, *J. Atmos. Sci.*, *65*, 3571–3583.

Schneider, T., and C. C. Walker (2008), Scaling laws and regime transitions of macroturbulence in dry atmospheres, *J. Atmos. Sci.*, *65*(7), 2153–2173.

Schneider, T., P. A. O'Gorman, and X. J. Levine (2010), Water vapor and the dynamics of climate changes, *Rev. Geophys.*, *48*, RG3001, doi:10.1029/2009RG000302.

Seidel, D. J., Q. Fu, W. J. Randel, and T. J. Reichler (2008), Widening of the tropical belt in a changing climate, *Nat. Geosci.*, *1*(1), 21–24.

Seo, K.-H., D. M. Frierson, and J.-H. Son (2014), A mechanism for future changes in Hadley circulation strength in CMIP5 climate change simulations, *Geophys. Res. Lett.*, *41*, 5251–5258, doi:10.1002/2014GL060868.

Vecchi, G. A., and B. J. Soden (2007), Global warming and the weakening of the tropical circulation, *J. Clim.*, *20*(17), 4316–4340.

Walker, C. C., and T. Schneider (2006), Eddy influences on Hadley circulations: Simulations with an idealized GCM, *J. Atmos. Sci.*, *63*(12), 3333–3350.